Video Article

Production of Metal Nanoparticles by Pulsed Laser-ablation in Liquids: A Tool for Studying the Antibacterial Properties of Nanoparticles

Matthew Ratti[1], Joseph J. Naddeo[1], Julianne C. Griepenburg[1], Sean M. O'Malley[1,2], Daniel M. Bubb[1,2], Eric A. Klein[2,3]

[1]Physics Department, Rutgers University-Camden

[2]Center for Computational and Integrative Biology, Rutgers University-Camden

[3]Biology Department, Rutgers University-Camden

Correspondence to: Eric A. Klein at eric.a.klein@rutgers.edu

URL: https://www.jove.com/video/55416
DOI: doi:10.3791/55416

Keywords: Bioengineering, Issue 124, Pulsed laser-ablation in liquids, nanoparticles, antimicrobial, *E. coli*, silver toxicity, post-irradiation, microbiology

Date Published: 6/2/2017

Citation: Ratti, M., Naddeo, J.J., Griepenburg, J.C., O'Malley, S.M., Bubb, D.M., Klein, E.A. Production of Metal Nanoparticles by Pulsed Laser-ablation in Liquids: A Tool for Studying the Antibacterial Properties of Nanoparticles. *J. Vis. Exp.* (124), e55416, doi:10.3791/55416 (2017).

Abstract

The emergence of multidrug-resistant bacteria is a global clinical concern leading some to speculate about our return to a "pre-antibiotics" era of medicine. In addition to efforts to identify novel small-molecule antimicrobial drugs, there has been great interest in the use of metal nanoparticles as coatings for medical devices, wound dressings, and consumer packaging, due to their antimicrobial properties. The wide variety of methods available for nanoparticle synthesis results in a broad spectrum of chemical and physical properties which can affect antibacterial efficacy. This manuscript describes the pulsed laser-ablation in liquids (PLAL) method to create nanoparticles. This approach allows for the fine tuning of nanoparticle size, composition, and stability using post-irradiation methods as well as the addition of surfactants or volume excluders. By controlling particle size and composition, a large range of physical and chemical properties of metal nanoparticles can be explored which may contribute to their antimicrobial efficacy thereby opening new avenues for antibacterial development.

Video Link

The video component of this article can be found at https://www.jove.com/video/55416/

Introduction

Nanoparticles (NPs) are generally defined as particles that have at least one dimension that is less than 100 nm in length. Traditional chemical NP synthesis methods typically require hazardous reducing agents, such as borohydrides and hydrazines. In contrast, laser ablation of solid metal targets immersed in a liquid medium (pulsed laser-ablation in liquids – PLAL) provides an environmentally friendly route for NP synthesis that satisfies all 12 of the Principles of Green Chemistry[1,2]. In PLAL, a submerged metal target is irradiated by repeated laser pulses. As the laser ablates the target, a dense plume of atomic clusters and vapor is released into the liquid medium wherein NPs rapidly coalesce. NPs produced by PLAL are finely dispersed in an aqueous medium and the size, polydispersity, and composition of the NPs can be easily controlled by varying the aqueous ablation liquid as well as laser parameters[1,2,3,4,5,6].

Nanoparticle characteristics can be tuned by adjusting a number of laser parameters, including: fluence, wavelength, and pulse duration (reviewed in reference[7]). Laser fluence is calculated as the pulse energy divided by the area of the laser spot on the target surface. The precise effects of fluence on the size and polydispersity of NPs are somewhat controversial. In general, it has been shown that for 'long' and 'ultra-short' pulsed laser systems there are low and high fluence regimes that produce negative and positive trends in size, respectively[8,9,10,11]. NP size distributions can be empirically measured using techniques such as dynamic light scattering and transmission electron microscopy (TEM), as described below.

The choice of laser wavelength can affect the physical mechanisms by which the NPs are formed. At shorter (ultraviolet) wavelengths, high energy photons are capable of breaking interatomic bonds[12]. This mechanism of photo-ablation is an example of a top-down NP synthesis because it results in the release of ultra-small fragments of material which tend to produce larger more polydisperse samples upon quenching in the submersion liquid[12,13,14]. In contrast, near-infrared ablation (λ = 1,064 nm) yields a bottom-up synthesis mechanism dominated by plasma ablation[12]. Laser absorption by the target frees electrons that collide with, and subsequently free, bound electrons. As collisions increase, the material is ionized, thus igniting a plasma. The surrounding liquid confines the plasma, enhances its stability, and further increases absorption[12]. As the expanding plasma is quenched by the confining liquid, NPs are condensed with various geometries[4,12,15].

The choice of laser pulse duration can further impact the NP-formation process. Commonly used long-pulsed lasers, with pulse durations greater than a few picoseconds, include all milli, micro, nano and some picosecond pulsed lasers. In this pulse-width regime, the laser pulse duration is longer than the electron-phonon equilibration time, which is typically on the order of a few picoseconds[4,16,17,18,19]. This results in the leaking

of energy into the surrounding ablation medium and the formation of NPs by thermal mechanisms such as thermionic emission, vaporization, boiling and melting[1,20].

The antibacterial activity of NPs is strongly influenced by particle size[21,22,23,24]. In order to enhance size reduction and monodispersity, the NPs can be irradiated a second time using a laser of a wavelength near the surface plasmon resonance (SPR) of the NP. The incident laser radiation is absorbed by the NP through excitation of the SPR. Fragmentation of the NP may occur through either thermal evaporation[25,26] or Coulomb explosion[27,28]. The photoexcitation raises the temperature of the NP above the melting point, resulting in the shedding of the outer layer of the particle. It has been shown that adding agents such as polyvinylpyrrolidone (PVP) or sodium dodecyl sulfate (SDS) to the solution can greatly enhance post-irradiation effects[5]. The impact of the addition of various solutes have been described in several reports[1,4,6]. The ease of manipulation of NP characteristics by PLAL affords a novel method to develop novel NP-based antimicrobials.

Protocol

1. Focusing the Nanosecond Laser and Measuring Fluence

1. **Assemble the ablation apparatus by placing a magnetic stir bar and a porous ablation stage inside a 50 mL glass beaker.**
   NOTE: The ablation stage consists of a 3.81 cm diameter, 1.6 mm thick stainless steel platform with ten 0.65 cm diameter holes and six 0.50 cm diameter holes drilled in the pattern illustrated in **Figure 1**. The purpose of these holes is to allow the liquid to move across the target so that particles do not accumulate immediately above the target. Insufficient mixing leads to deleterious interactions between the laser and the already-formed particles. Additionally, three #29 (8-32) tapped holes are located near the perimeter of the platform to accept set screws which serve as legs to raise the platform and provide space for a magnetic stir bar (**Figure 1A**).
   1. Place the beaker on a magnetic stir plate and set the stir plate upon an xy-translation stage to enable movement of the target during ablation (**Figure 1A**).
2. Set the Nd:YAG laser to operate at the fundamental wavelength of 1,064 nm, with a pulse duration of 5 ns, and a pulse repetition rate of 10 Hz. Measure the energy per pulse with a laser power and energy meter. The energy required is 240-250 mJ.
3. Focus the beam beneath the target on the ablation stage using a 250 mm focal length converging lens (NA = 0.05).
   NOTE: The incoming beam has a radius of 4.025 mm and a lens height of 161 mm is required to attain the desired spot size. The optimal spot size is determined empirically. A larger spot size is utilized to reduce the effect of shielding by NPs present in solution. This is balanced with the fact that increasing spot size requires higher energy to maintain adequate fluence.
4. Determine the spot size by placing a metal target (see section 2) on the stage and ablating with several laser pulses. View the ablated target together with a micrometer slide on a CCD camera-equipped light microscope (4X objective) to measure the spot size (**Figure 1A**).
   NOTE: For the apparatus here, the ablation system yields a spot size with a mean area of 5.51 mm^2. The spot size remains in this range for each ablation.
5. Calculate fluence by dividing the pulse energy by the spot area. For the apparatus here, the fluence is 4.80 J/cm^2.

2. Synthesis of Silver Nanoparticles by Pulsed Laser-ablation in Liquid

1. Weigh a flat silver target using a microbalance to obtain the pre-ablation mass.
2. Adhere the silver target to the porous stage using double-sided carbon tape. Add 40 mL of ablation liquid to the beaker (**Figure 1A**). The liquid height above the target is 11 mm.
   NOTE: Typical ablation liquids are aqueous solutions containing either 60 mM SDS or 2 mM PVP to enhance monodispersity.
3. Under constant stirring, move the computer-controlled motorized xy-stage in an elliptical pattern (dimensions: major axis = 2.09 cm, minor axis = 0.956 cm, area = 1.57 cm^2) at a speed of 0.42 cm/s and ablate the target for 20-40 min.
   NOTE: The concentration of NPs increases with longer ablation times. Ensure that the stirring is sufficiently vigorous to keep the NP concentration uniform throughout the solution to minimize shielding effects[7].

3. Characterizing Metal Nanoparticles

1. Collect the nanoparticle solution from the beaker by decanting. Confirm the presence of nanoparticles by measuring their UV-visible light spectra (200-1,100 nm).
   NOTE: The NPs have a peak-absorption at the surface plasmon resonance (SPR) wavelength. For silver, the SPR is centered at 400 nm. Highly concentrated NP solutions require dilution prior to measuring the UV-VIS spectrum to ensure that the absorbance readings remain within the linear range of the spectrophotometer.
2. **Measure the hydrodynamic diameter of the NPs by dynamic light scattering (DLS) utilizing a number distribution analysis method[29].**
   1. Dilute the NP solution 1:40 in the ablation solution and pipette 1 mL into a 1 cm plastic cuvette. Utilizing a measurement angle of 180°, measure the light scattering at a wavelength of 633 nm to determine the NP diameter according to the Stokes-Einstein equation:
      $$d = \frac{kT}{3\pi\eta D}$$
      where d is the hydrodynamic radius, k is Boltzmann's constant, T is absolute temperature, η is viscosity, and D translational diffusion coefficient or velocity of Brownian motion.
3. **Confirm NP size and shape using transmission electron microscopy (TEM)[30].**
   NOTE: The hydrodynamic diameter measured using DLS is larger than the size measured using TEM due to the solvent layer surrounding the NPs.

1. Dilute the NP solution 1:40 in double-distilled water to remove any excess additives (*e.g.* SDS or PVP) that may interfere with imaging. Drop 2 µL of the solution onto a copper TEM grid pre-coated with lacey/thin carbon film (commercially available; see the Materials List) and dry overnight at room temperature under vacuum in a desiccator.
2. Image the NPs to assess size and shape as described in reference[30].

4. **To calculate the NP concentration, dislodge any loosely attached NPs from the ablated metal target (step 2.3) by placing the target in a sonicating water bath containing distilled water for 1 min.**
   1. Dry the target under a stream of compressed air for 1 min. Measure the mass of the target on a microbalance. Quantify the mass of NPs in solution as the difference in weight before and after ablation, which is assumed to be the result of ejection of metal nanoparticles into the solution.

4. Post-irradiation

1. Dilute the NPs to a maximum concentration of 100 µg/mL in the same ablation solution used in 2.2. This concentration limit is critical to ensure uniform irradiation.
2. Transfer 15-17 mL of the diluted NPs to a quartz cuvette containing a stir bar (**Figure 1B**). Place the cuvette on a magnetic stir-plate aligned parallel with the incoming laser.
3. Use a Nd:YAG laser system to produce 25 ps 532 nm laser pulses and a 75 mm focal-length lens to focus the laser on the center of the solution. Irradiate the solution for 30 min to multiple hours, depending on the desired size.
   NOTE: The total energy delivered depends on the concentration of the solution and time of irradiation and can range from 0.5 mJ to 3.5 mJ. For the apparatus here, 30 min of post-irradiation of a transparent, low concentration sample (<50 µg/mL) yields silver NPs with a diameter of 10 nm.

5. Measuring the Antibacterial Properties of the Nanoparticles

NOTE: The toxicity of silver NPs against both Gram-positive (*Bacillus subtilis*) and Gram-negative (*Escherichia coli*) was tested[31]. The method is easily adapted to any species; however the efficacious dose of nanoparticles may vary considerably and must be determined empirically. Here, *E. coli* is used as the model system for the description of the method.

1. Grow *E. coli* cultures (strain MG1655) overnight at 37 °C in Luria Broth (LB) containing 10 g/L Bacto tryptone, 5 g/L yeast extract, and 10 g/L sodium chloride. Dilute the overnight cultures to an optical density (λ = 600 nm) of 0.01 in fresh LB.
2. If the NPs were synthesized in ablation media containing additives (*e.g.* SDS or PVP), add the respective chemical to the LB such that the concentration remains constant upon adding the NPs.
   NOTE: For example, in a typical experiment a silver target is ablated into a 60 mM SDS solution to yield a 100 µg/mL solution of NPs. If the final concentration of NPs in the culture media is 10 µg/mL, prepare LB containing 6 mM SDS (*i.e.* 1/10 the concentration of SDS in the ablation liquid). There is no negative effect on the bacteria's growth when using these concentrations. This is shown in the -AgNP control in **Figure 3**.
3. Add the NPs to the diluted cultures at concentrations ranging from 0-50 µg/mL and grow the cultures with shaking at 37 °C for an additional 2 h. As a positive control for toxicity, treat *E. coli* with an antibiotic (*e.g.* 30 µg/mL kanamycin).
4. After the 2 h incubation, serially dilute the culture samples 1:10 into fresh LB and spot 10 µL drops of each dilution onto LB agar plates. Typically, 10^4-10^8 fold dilutions are sufficient to see individual colonies.
5. Once the droplets have been absorbed, incubate the plates overnight at 37 °C and count colony forming units (cfu) the following morning.

Representative Results

Using silver targets, the laser parameters described above, and 60 mM SDS in the ablation liquid, silver NPs are generated with the characteristic UV-VIS absorbance at the SPR (**Figure 2A**). TEM and DLS measurements reveal a mean NP diameter of approximately 25 nm before post-irradiation (**Figure 2B**). Ablation of the silver target for 30 min typically yields an NP concentration of 200 µg/mL. In assessing the antimicrobial toxicity of silver NPs, 15 µg/mL strongly inhibits *E. coli* growth (**Figure 3**).

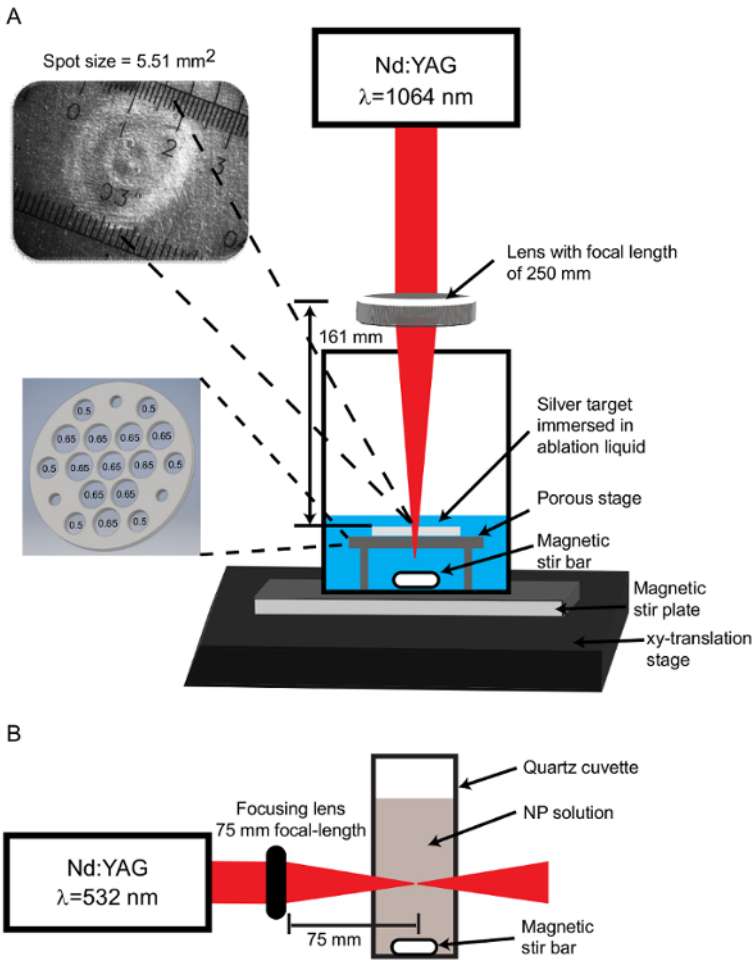

Figure 1: Apparatus configurations. (**A**) For the PLAL process, the Nd:YAG laser operating at a wavelength of 1,064 nm is focused through a 250 mm focal length lens to produce a spot size of 5.51 mm^2 on the target stage. The spot size image is captured using a CCD camera coupled with an optical microscope. The ablation target is set on a porous stage with ten 0.65 cm diameter holes and six 0.50 cm diameter holes. An additional 3 holes are tapped for set screws which function as legs to support the stage above the stir bar. (**B**) For post-irradiation, the Nd:YAG laser output is set to 532 nm and focused through a 75 mm focal-length lens onto the center of a quartz cuvette containing NPs. Please click here to view a larger version of this figure.

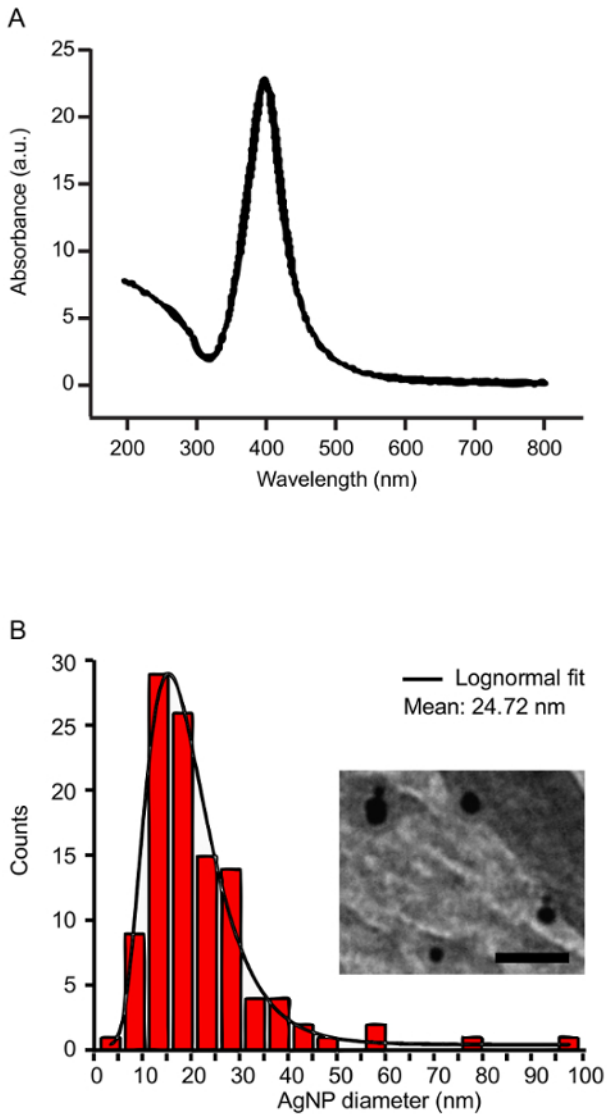

Figure 2: Characterization of silver nanoparticles. (**A**) The UV-VIS spectrum of silver NPs shows a characteristic peak at the SPR wavelength (400 nm). (**B**) The size distribution of the silver NPs before post-irradiation was measured by TEM. The inset shows a representative TEM image of AgNPs (85,000X magnification, Scale bar = 100 µm). Please click here to view a larger version of this figure.

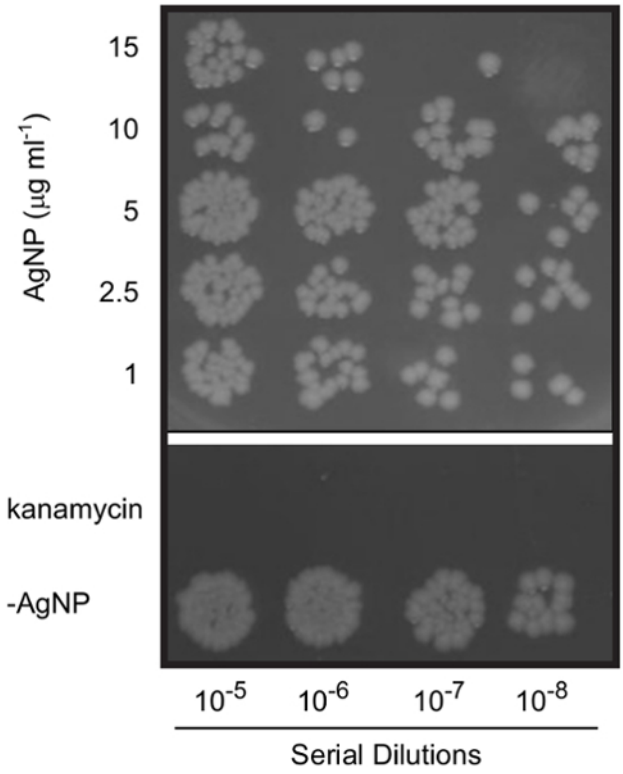

Figure 3. Antimicrobial effects of silver nanoparticles. *E. coli* cells were treated for 2 h with varying concentrations of silver NPs. Serial dilutions of cultures were plated on LB-agar to determine bacterial viability. Cells were treated with 30 µg/mL kanamycin as a positive control. Note that the cells not receiving AgNPs (-AgNP sample) were grown in the presence of 6 mM SDS to ensure that the surfactant did not independently result in toxicity. The figure is a composite of colonies on two plates from the same experiment and is a representative result (n = 5). Please click here to view a larger version of this figure.

Discussion

Reproducible antimicrobial effects of NPs require consistent production of NPs with similar sizes and concentrations. Therefore, it is critical to standardize laser parameters including fluence, wavelength, and pulse duration. While dynamic light scattering is an easy and rapid method for estimating NP size, accurate quantification of the size distribution requires direct measurement by TEM. As each laser beam has distinct characteristics in terms of mode profile and divergence, it is critical to employ an empirical process to yield the optimal fluence and liquid height over the target. Since the size of the nanoparticles can be adjusted by post-irradiation, the efficiency of particle production can be optimized through target mass-loss and optical density measurements.

In contrast to conventional chemical synthesis methods, laser ablation in liquids has the advantage of producing nanoparticles in either pure water or a surfactant solution. There are no precursor compounds to contaminate the cultures and act as interferents. Researchers can produce the nanoparticles in their laboratory in a short period of time for immediate use. The technique is highly reproducible and does not require specialized training or personnel. However, it is important to note the limitations of this method. First, the diversity in shapes of the nanoparticles that are produced by laser ablation in liquids can vary over a wide range. If one is required to target particular aspect ratios or other shape parameters, highly iterative processing would be required if it is possible at all. Perhaps the most significant limitation of this technique is that experiments which require large masses of nanoparticles will be difficult. Gram-scale synthesis can occur, but it is challenging and requires specialized laser equipment[32,33,34].

It is important to note that many metal NPs are light-sensitive. Indeed, irradiation of silver nanoparticles with visible light results in increased antibacterial toxicity[31]. The enhanced efficacy is due to an increase in silver ion release from the NPs. Therefore, it is important to consider whether to perform the PLAL method and store the resulting NPs protected from light.

Lastly, the choice of surfactants and volume-excluders (*e.g.* SDS and PVP) to decrease NP size is critical when studying the antimicrobial potency of NPs. It is important to perform control experiments to ensure that the additives are not toxic on their own. For example, *E. coli* tolerates SDS at concentrations up to 10 mM; however, *B. subtilis* is much more sensitive[31]. Therefore, when working with *B. subtilis,* non-toxic concentrations of PVP (2 mM) can be added to the ablation liquid to obtain 25 nm particles.

Laser ablation in liquids along with post-irradiation can be used to produce nanoparticle distributions with a range of dispersities and sizes. This will facilitate studies with different bacteria, metals, and even alloys. The use of PLAL for nanoparticle synthesis provides a novel method for developing antimicrobial NPs to combat the ever-growing challenge of antibacterial resistance.

Disclosures

The authors have nothing to disclose.

Acknowledgements

This work was supported by the National Science Foundation (NSF awards CMMI-0922946 to D.B., CMMI-1300920 to D.B. and S.O'M., and CMMI-1531789 to S.O'M., D.B., and E.A.K.) and a Busch Biomedical Research Grant to E.A.K. and S.O'M.

References

1. Amendola, V., & Meneghetti, M. What controls the composition and the structure of nanomaterials generated by laser ablation in liquid solution? *Phys Chem Chem Phys.* **15** (9), 3027-3046 (2013).
2. Anastas, P., & Eghbali, N. Green chemistry: principles and practice. *Chem Soc Rev.* **39** (1), 301-312 (2010).
3. Mafune, F., Kohno, J.-y., Takeda, Y., Kondow, T., & Sawabe, H. Formation of Gold Nanoparticles by Laser Ablation in Aqueous Solution of Surfactant. *J Phys Chem B.* **105** (22), 5114-5120 (2001).
4. Rao, S. V., Podagatlapalli, G. K., & Hamad, S. Ultrafast laser ablation in liquids for nanomaterials and applications. *J Nanosci Nanotechnol.* **14** (2), 1364-1388 (2014).
5. Tsuji, T. *et al.* Preparation of silver nanoparticles by laser ablation in polyvinylpyrrolidone solutions. *Appl Surf Sci.* **254** (16), 5224-5230 (2008).
6. Zeng, H. *et al.* Nanomaterials via laser ablation/irradiation in liquid: a review. *Adv Funct Mater.* **22** (7), 1333-1353 (2012).
7. Naddeo, J. J. *et al.* Antibacterial Properties of Nanoparticles: A Comparative Review of Chemically Synthesized and Laser-Generated Particles. *Adv. Sci. Eng. Med.* **7** (12), 1044-1057 (2015).
8. Elsayed, K. A., Imam, H., Ahmed, M. A., & Ramadan, R. Effect of focusing conditions and laser parameters on the fabrication of gold nanoparticles via laser ablation in liquid. *Opt. & Laser Tech.* **45** 495-502 (2013).
9. Kabashin, A. V., & Meunier, M. Synthesis of colloidal nanoparticles during femtosecond laser ablation of gold in water. *J Appl Phys.* **94** (12), 7941-7943 (2003).
10. Nichols, W. T., Sasaki, T., & Koshizaki, N. Laser ablation of a platinum target in water. I. Ablation mechanisms. *J Appl Phys.* **100** (11), 114911 (2006).
11. Povarnitsyn, M. E., Itina, T. E., Levashov, P. R., & Khishchenko, K. V. Mechanisms of nanoparticle formation by ultra-short laser ablation of metals in liquid environment. *Phys Chem Chem Phys.* **15** (9), 3108-3114 (2013).
12. Mortazavi, S. Z., Parvin, P., Reyhani, A., Golikand, A. N., & Mirershadi, S. Effect of Laser Wavelength at IR (1064 nm) and UV (193 nm) on the Structural Formation of Palladium Nanoparticles in Deionized Water. *J Phys Chem C.* **115** (12), 5049-5057 (2011).
13. Kim, J., Reddy, D. A., Ma, R., & Kim, T. K. The influence of laser wavelength and fluence on palladium nanoparticles produced by pulsed laser ablation in deionized water. *Solid State Sci.* **37** 96-102 (2014).
14. Mortazavi, S. Z., Parvin, P., Reyhani, A., Mirershadi, S., & Sadighi-Bonabi, R. Generation of various carbon nanostructures in water using IR/UV laser ablation. *J Phys D: Appl Phys.* **46** (16), 165303 (2013).
15. Hunter, B. M. *et al.* Highly active mixed-metal nanosheet water oxidation catalysts made by pulsed-laser ablation in liquids. *J Am Chem Soc.* **136** (38), 13118-13121 (2014).
16. Momma, C. *et al.* Short-pulse laser ablation of solid targets. *Opt Commun.* **129** (1), 134-142 (1996).
17. Sonntag, S., Roth, J., Gaehler, F., & Trebin, H. R. Femtosecond laser ablation of aluminium. *Appl Surf Sci.* **255** (24), 9742-9744 (2009).
18. Yamashita, Y., Yokomine, T., Ebara, S., & Shimizu, A. Heat transport analysis for femtosecond laser ablation with molecular dynamics-two temperature model method. *Fusion Eng Des.* **81** (8), 1695-1700 (2006).
19. Zhigilei, L. V., Lin, Z., & Ivanov, D. S. Atomistic modeling of short pulse laser ablation of metals: connections between melting, spallation, and phase explosion. *J Phys Chem C.* **113** (27), 11892-11906 (2009).
20. Schmidt, M. *et al.* Lasers in Manufacturing 2011 - Proceedings of the Sixth International WLT Conference on Lasers in Manufacturing Metal Ablation with Short and Ultrashort Laser Pulses. *Physics Procedia.* **12** 230-238 (2011).
21. Azam, A., Ahmed, A. S., Oves, M., Khan, M. S., & Memic, A. Size-dependent antimicrobial properties of CuO nanoparticles against Gram-positive and-negative bacterial strains. *Int. J. Nanomed.* **7** 3527-3535 (2012).
22. Ivask, A. *et al.* Size-dependent toxicity of silver nanoparticles to bacteria, yeast, algae, crustaceans and mammalian cells in vitro. *PLoS One.* **9** (7), e102108 (2014).
23. Kim, T. H. *et al.* Size-dependent cellular toxicity of silver nanoparticles. *J Biomed Mater Res A.* **100** (4), 1033-1043 (2012).
24. Raghupathi, K. R., Koodali, R. T., & Manna, A. C. Size-dependent bacterial growth inhibition and mechanism of antibacterial activity of zinc oxide nanoparticles. *Langmuir.* **27** (7), 4020-4028 (2011).
25. Plech, A., Kotaidis, V., Gresillon, S., Dahmen, C., & von Plessen, G. Laser-induced heating and melting of gold nanoparticles studied by time-resolved x-ray scattering. *Phys Rev B.* **70** (19), 195423 (2004).
26. Takami, A., Kurita, H., & Koda, S. Laser-Induced Size Reduction of Noble Metal Particles. *J Phys Chem B.* **103** (8), 1226-1232 (1999).
27. Kamat, P. V., Flumiani, M., & Hartland, G. V. Picosecond Dynamics of Silver Nanoclusters. Photoejection of Electrons and Fragmentation. *J Phys Chem B.* **102** (17), 3123-3128 (1998).
28. Yamada, K., Tokumoto, Y., Nagata, T., & Mafune, F. Mechanism of laser-induced size-reduction of gold nanoparticles as studied by nanosecond transient absorption spectroscopy. *J Phys Chem B.* **110** (24), 11751-11756 (2006).
29. Pecora, R. Dynamic Light Scattering Measurement of Nanometer Particles in Liquids. *J. Nanoparticle Res.* **2** (2), 123-131 (2000).
30. Pyrz, W. D., & Buttrey, D. J. Particle size determination using TEM: a discussion of image acquisition and analysis for the novice microscopist. *Langmuir.* **24** (20), 11350-11360 (2008).
31. Ratti, M. *et al.* Irradiation with visible light enhances the antibacterial toxicity of silver nanoparticles produced by laser ablation. *Appl Phys A.* **122** (4), 1-7 (2016).

32. Sajti, C. L., Sattari, R., Chichkov, B. N., & Barcikowski, S. Gram Scale Synthesis of Pure Ceramic Nanoparticles by Laser Ablation in Liquid. *J Phys Chem C.* **114** (6), 2421-2427 (2010).
33. Streubel, R., Barcikowski, S., & Gokce, B. Continuous multigram nanoparticle synthesis by high-power, high-repetition-rate ultrafast laser ablation in liquids. *Opt Lett.* **41** (7), 1486-1489 (2016).
34. Streubel, R., Bendt, G., & Gokce, B. Pilot-scale synthesis of metal nanoparticles by high-speed pulsed laser ablation in liquids. *Nanotechnology.* **27** (20), 205602 (2016).

